ELSEVIER

Biochimica et Biophysica Acta 1275 (1996) 227–236

BBA Biochimica et Biophysica Acta

Studies of light-induced nickel EPR signals in hydrogenase: comparison of enzymes with and without selenium

Milagros Medina [a,1], E. Claude Hatchikian [b], Richard Cammack [a,*]

[a] *Centre for the Study of Metals in Biology and Medicine, Division of Life Sciences, King's College, Campden Hill Road, London W8 7AH, UK*
[b] *Laboratoire de Chimie Bacterienne, CNRS-BP 71, 13277 Marseille Cedex 9, France*

Received 4 January 1996; accepted 10 January 1996

Abstract

Upon reduction under hydrogen-argon atmosphere, the nickel-hydrogenases generally show a characteristic rhombic EPR spectrum which is known as Ni-C. Illumination of this state at temperatures below 60 K has previously been shown to cause the disappearance of the Ni-C signal and the simultaneous appearance of two overlapping signals, here referred to as Ni-L1 and Ni-L2, which revert to the Ni-C state at higher temperatures. These phenomena have been compared in three nickel-containing hydrogenases, the [NiFe]-hydrogenases from *Desulfovibrio gigas* and *Desulfovibrio fructosovorans*, and the selenium-containing soluble [NiFeSe]-hydrogenase from *Desulfomicrobium baculatum*. Significant differences were observed between these enzymes. (1) The Ni-C, Ni-L1 and Ni-L2 EPR spectra were almost identical for *D. gigas* and *D. fructosovorans* hydrogenases, but the rates of photoconversion of Ni-C to Ni-L1 were different, being about 5 times slower for *D. fructosovorans* than for *D. gigas* in H_2O. (2) The kinetic isotope effect in $^2H_2O/H_2O$ was a factor of thirty in *D. gigas*, but only two in *D. fructosovorans*. *Dm. baculatum* hydrogenase showed almost no kinetic isotope effect on the Ni-C to Ni-L1 conversion, but an effect on the conversion of Ni-L1 to Ni-L2. The kinetic isotope effects indicate that the processes involve the movement of a hydrogen nucleus. (3) The Ni-L1 species converted to into Ni-L2 in the dark at a rate that was virtually temperature-independent below 30 K, indicative of a proton tunnelling process. (4) The conversion of Ni-L1 to Ni-L2 was partly reversed by light in *Dm. baculatum* hydrogenase, but not in the [NiFe]-hydrogenases. (5) Prolonged illumination of the three enzymes induced the appearance of a third light-induced signal, Ni-L3. The new signal was rhombic, with features at $g = 2.41$, 2.16 (the third component being unresolved) in the [NiFe]-hydrogenases and $g = 2.48$, 2.16, 2.03 for the [NiFeSe]-enzyme. (6) Splittings caused by by spin-spin interactions with [4Fe-4S] clusters were detected for all the illuminated signals, Ni-L1, Ni-L2 and Ni-L3. These were quantitatively different for the three enzymes. (7) Broadening of the Ni-C signals in H_2O compared with ^2H_2O was observed in the g_1 and g_2 components of *D. gigas* and *D. fructosovorans* hydrogenases, but not for *Dm. baculatum*. This broadening effect was not seen with any of the Ni-L species. These comparative effects are discussed in terms of subtle differences in the structure and protein environment of the nickel site, and access to exchangeable hydrons.

Keywords: Hydrogenase; Photochemistry; Electron paramagnetic resonance spectroscopy; Nickel; Sulphate-reducing bacteria

1. Introduction

Hydrogenases are the metalloenzymes that carry out the reversible two-electron oxidation of dihydrogen. They are divided into different classes according to their metal content. One group consists of the enzymes possessing only iron-sulphur clusters ([Fe]-hydrogenases) [1]. Other hydrogenases contain nickel in addition to iron ([NiFe]-hydrogenases) [2,3]. The [NiFe]-hydrogenases are the most commonly found hydrogenases in many prokaryotic organisms [4], including the sulphate-reducing bacteria [5] where they play a central role in energy metabolism. In the [NiFe]-hydrogenases, the nickel centre is believed to be the site at which hydrogen binds [3,6]. In these hydrogenases it has been proposed that the iron-sulphur clusters serve as secondary electron carriers [7,8]. Among the hydrogenases containing nickel there is a class of enzymes that contain selenium as well ([NiFeSe]-hydrogenases) [9]. In these

Abbreviations: c.w., continuous wave; *D.*, *Desulfovibrio*; *Dm.*, *Desulfomicrobium*; ENDOR, electron nuclear double resonance; EPR, electron paramagnetic resonance; T_1, spin-lattice relaxation time.

* Corresponding author. Fax: +44 171 3334500.
[1] Present address: Departamento de Bioquimica y Biologia Molecular y Celular, Facultad de Ciencias, Universidad de Zaragoza, 50009-Zaragoza, Spain.

PII S0005-2728(96)00007-2

enzymes, the selenium is generally present as a single selenocysteine residue, which spectroscopic studies have shown to be one of the ligands to nickel [10–12].

D. gigas [NiFe]-hydrogenase has a molecular mass of 89 kDa with two subunits of molecular mass 63 and 26 kDa, respectively. It has a high content of iron and labile sulphide as well as approx. 1 nickel atom per molecule [2,13]. The iron and sulphide are arranged as two [4Fe-4S] and one [3Fe-4S] clusters [8]. *D. gigas* hydrogenase has been crystallised, and its structure determined [14,15]. As predicted from amino acid sequences [16], the three iron-sulphur clusters are located in the 26 kDa subunit while the Ni atom is in the large subunit. The distance between the Ni site and the nearest [4Fe-4S] cluster is about 1.2 nm. An unexpected feature of the structure is the presence of another metal ion, 0.27 nm from the nickel site, which was assigned to an iron atom [15].

EPR spectroscopy has been used extensively to probe the metal centres in hydrogenases. The oxidized form of *D. gigas* [NiFe]-hydrogenase displays an almost isotropic EPR signal centred around $g = 2.02$, due to the $[3Fe\text{-}4S]^{1+}$ cluster, and two rhombic signals, with g-factors between $g = 2.01$ and 2.34 [17], which have been assigned to low-spin Ni^{III} in different coordination states. One of these two signals, designated Ni-A, at $g = 2.32$, 2.23, 2.01 is usually the most prominent [18]. The other, Ni-B, is normally present as a minor species, typically less than 10% in the enzyme as purified. The oxidized enzyme is unreactive with hydrogen directly, requiring reduction to become active. The form of the enzyme showing the Ni-B signal is able to react immediately on reduction, and is called the 'ready' state, while the form showing the Ni-A signal can react only after prolonged incubation (hours) with reducing agents and is termed the 'unready' state [19]. On reduction these signals disappear, yielding an EPR-silent state. A third signal, Ni-C, is associated with a reduced form of the activated enzyme [20]; this signal has been identified as due to nickel by substitution with ^{61}Ni and observation of the hyperfine structure [17]. Further reduction of the enzyme to lower redox potentials causes this signal to disappear. The amount of the enzyme giving the Ni-C signal is a function of redox potential and pH [7].

The Ni-A and Ni-B signals have been observed in some, but not all nickel-containing hydrogenases [21]; in particular they are absent from [NiFeSe]-hydrogenases. By contrast the Ni-C signal has been observed in most nickel-hydrogenases. The g-factors of the signal are remarkably consistent, $g = 2.19$, 2.14, 2.01 for the [NiFe]-hydrogenases, and slightly higher ($g = 2.21$, 2.16, 2.01) for the [NiFeSe]-hydrogenases. At lower temperatures (below 10 K), and at redox potentials where the [4Fe-4S] centres are also reduced, the spectrum changes into a fast-relaxing species with a complex lineshape. This complex spectrum has been interpreted as due to the influence of exchange and dipolar interactions with the paramagnetic iron-sulphur clusters [7,22]. Various lines of evidence suggest that the form of nickel giving the Ni-C signal is the active form, which reacts with hydrogen. For example, the linewidth of the spectrum is broader when the enzyme is prepared in H_2O than in ^2H_2O [23]. The signal shows hyperfine couplings with exchangeable ^2H when prepared in ^2H_2O [24], as well as ^1H hyperfine splittings [25,26].

Another significant property of the hydrogenase state giving the Ni-C signal is its sensitivity to light. As first demonstrated in *Chromatium vinosum* hydrogenase by Van der Zwaan et al. [23], the enzyme undergoes a photoconversion in the frozen state at 77 K, to a species, with different g-factors, which is described variously as Ni-L or Ni-C*. Here for consistency with other literature [26] we will use the term Ni-L. Similar light sensitivity has been observed in hydrogenases from other species, including *Wolinella succinogenes* [23], *D. gigas* [7], *Thiocapsa roseopersicina* [26,27], and *Methanococcus voltae* [28]. Van der Zwaan et al. [23] also demonstrated that the rate of photoconversion of *C. vinosum* hydrogenase was significantly (6-fold) slower in ^2H_2O than in H_2O. The photochemical conversion of Ni-C to Ni-L species is reversed by annealing the sample near 200 K [23,26].

These properties of the Ni-C signal have been taken as evidence that an exchangeable hydrogen atom must be in the direct coordination sphere of Ni-C, and further, that the nickel site is the active site of the enzyme, which interacts with dihydrogen and hydrons (i.e., hydrogen or deuterium ions). However, some differences between enzymes have been noted. For example, the Ni-C signal in the [NiFeSe]-hydrogenase in *M. voltae* has been reported not to show broadening in H_2O compared with ^2H_2O [28]. Photoconversion of the Ni-C signal in *C. vinosum* hydrogenase was found to induce two different EPR signals at low temperatures [23]. Therefore it is instructive to compare the properties described above, for different types of [NiFe]-hydrogenases, to see which properties are common to all enzymes and others that may not be relevant to the catalytic mechanism. In this paper we compare the properties of the [NiFe] periplasmic hydrogenases from *D. gigas* and *D. fructosovorans*, and the [NiFeSe]-soluble hydrogenase from *Dm. baculatum* and with results reported by other investigators for [NiFe]-hydrogenases purified from other sources.

D. fructosovorans contains a [NiFe]-hydrogenase which shows similarities with the enzyme from *D. gigas*. The amino acid sequences are highly homologous [29]. The EPR properties of the enzyme are consistent with the presence of Ni, [3Fe-4S] and [4Fe-4S] clusters [30], and show the presence of Ni-A, Ni-B and Ni-C with almost identical g-factors to those of *D. gigas*. However, the *D. fructosovorans* enzyme appears to be more easily converted to the ready state, and a higher proportion of the EPR-detectable nickel, in the enzyme as prepared, is present as Ni-B [30].

The soluble hydrogenase from *Desulfomicrobium baculatum* (formerly *D. desulfuricans*, strain Norway 4) consists of two subunits of 56 kDa and 29 kDa. It appears to

contain [4Fe-4S] clusters, but no [3Fe-4S] cluster, and selenium, in quantities equivalent to nickel [31,32]. The purified enzyme showed no EPR signals in the oxidized state. An EPR signal due to a rapidly-relaxing species, presumably the [4Fe-4S] cluster(s), with $g = 2.03$, 1.89, 1.86 was observed in the reduced protein, together with a weaker spectrum from a slower-relaxing species at $g =$ 2.215, 2.16, 2.01 assigned to nickel, analogous to Ni-C in *D. gigas* hydrogenase.

2. Materials and methods

The periplasmic hydrogenases from *D. gigas* and *D. fructosovorans*, and the soluble hydrogenase from *Dm. baculatum* were purified as described previously [13,30,32]. For the *D. gigas* hydrogenase samples it was observed that only about 40% of the nickel present in the enzyme as purified was EPR detectable, of which less than 2% was Ni-B. This effect was noted in earlier studies [33]. For the *D. fructosovorans* hydrogenase, the purified enzyme also showed just 40% of its nickel content as EPR detectable in the oxidized state, 24% as Ni-B and 16% as Ni-A. Samples were prepared in 50 mM MES buffer (pH 6.5), in order to enhance the amount of Ni-C signal produced. The samples in ^2H_2O were prepared by diluting oxidized enzyme with buffer made with ^2H_2O (50 mM MES, p^{2}H 6.5), and then concentrating by ultrafiltration through Centricon 30 microconcentrators (Amicon), at 4°C. The cycle was repeated three times, to give a final buffer or ^2H_2O enrichment of 99%.

EPR spectra were recorded on a Bruker ESP300 spectrometer with an Oxford Instruments ESR900 helium flow cryostat, using a TE102 cavity at X-band (9.3 GHz) and a split-ring resonator at S-band (4 GHz) frequencies. The spin concentration due to the nickel was determined using 1 mM Cu^{II}-EDTA as standard. EPR spectra of the standard and sample were recorded at a non-saturating microwave power and at temperatures above 100 K (to avoid interference from $[4Fe\text{-}4S]^{1+}$ and $[3Fe\text{-}4S]^{1+}$ signals), under identical instrument settings. The spin concentrations were then obtained by comparison of the double integral of the sample and standard spectra. EPR spectral simulations were performed using the program 'EPR' written by Dr. F. Neese (University of Konstanz, Germany), which represents a first-order solution to the spin hamiltonian, and allows simulation of the overlapping contributions from several distinct non-interacting paramagnets.

The hydrogenases were converted into redox states in which the nickel was in the Ni-C form and the [4Fe-4S] clusters were reduced to varying extents, in a cell designed for small volumes [34]. The enzyme was equilibriated under different partial pressures of oxygen-free, water-saturated hydrogen or argon gases at 25°C and pH 6.5 (50 mM MES), in the presence of trace amounts of methyl viologen (< 2 μM). For the samples in H_2O, hydrogenase was activated by reduction under H_2 gas overnight, after which the potential was adjusted by flushing the sample with water-saturated argon. The changes in redox potential were followed with a platinum electrode fitted in the base of the redox cell and a calomel reference electrode connected to a saturated KCl bridge and, calibrated against a quinhydrone standard. The maximum Ni-C signals were obtained at potentials between −360 and −390 mV. Samples were anaerobically transferred into EPR tubes, connected to the redox cell through a lateral arm, with a gas-tight microsyringe and then rapidly frozen at 77 K. Samples in ^2H_2O were reduced and activated under argon flow by adding sodium dithionite in ^2H_2O 100 mM Tris/^{2}HCl buffer p^{2}H 9 and then flushed with argon till the desired redox potential was achieved, then transferred into EPR tubes as before. It was found that the electrode response became sluggish at high protein concentrations, presumably due to coating of the electrodes, so the EPR spectra were taken as the final criterion that a good sample had been produced. Typically it was found that the concentration of the EPR-detectable Ni-C species, which is an intermediate state in the reduction of hydrogenase, represented 20–30% of the total enzyme concentration, i.e., 50–75% of the EPR-detectable nickel in the oxidized enzyme. Spectra recorded at temperatures below 10 K showed splitting of the Ni-C due to spin-spin interactions with [4Fe-4S] clusters [22]. Since the redox potential for complete reduction of the clusters is lower than that for the appearance of the Ni-C signal, the spectra contained both the normal rhombic ('unsplit') spectrum of the isolated Ni-C species, and the complex ('split') spectrum due to molecules in which the [4Fe-4S] clusters were reduced [22]. The proportion of the split and unsplit Ni-C signals could be adjusted by means of the redox potential [7].

Illumination of samples was carried out in the helium cryostat, at the desired temperatures, by means of a 150 W Barr and Stroud fibre-optic light source directed into the TE102 cavity through a stub waveguide for light access. Samples giving either split Ni-C or unsplit Ni-C species were illuminated at each of the temperatures 60 K, 30 K or 5 K. In kinetic studies, comparing for example $H_2O/^2H_2O$, *D. gigas*/*D. fructosovorans*/*Dm. baculatum*, samples were run sequentially while the illumination conditions and sample concentrations were held constant.

3. Results

3.1. Occurrence of three light-induced signals, Ni-L1, Ni-L2 and Ni-L3

Illumination of the unsplit Ni-C signal of *D. gigas* hydrogenase, at temperatures below 60 K, caused the disappearance of the single Ni-C signal and the simultaneous appearance of two overlapping signals [35], here referred to as Ni-L1 and Ni-L2. These light-induced signals

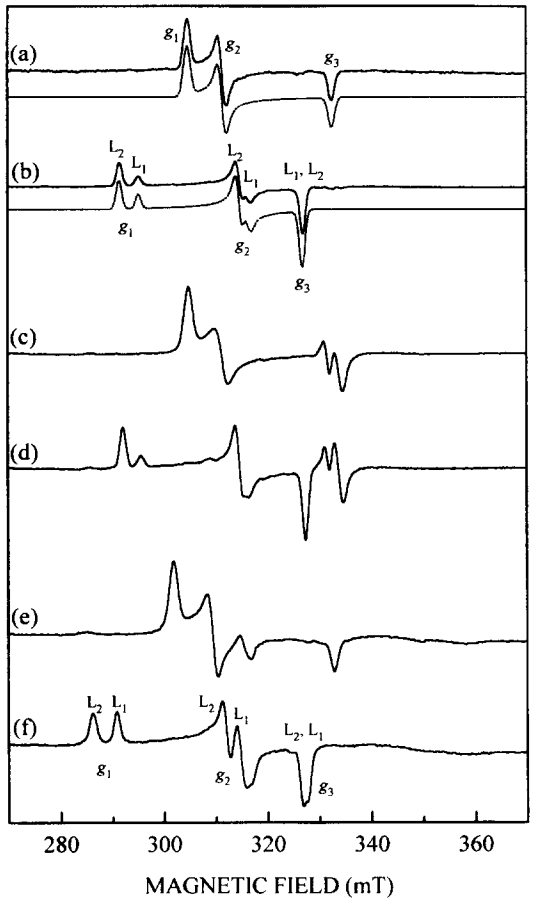

Fig. 1. Light-induced transitions of the Ni-C EPR signal of H_2-*reduced hydrogenase*. (a) Enzyme from *D. gigas* after reduction with hydrogen and subsequent treatment with argon. Ni-C concentration, 67 μM. (b) Spectrum obtained after illumination of the same sample for 3 min at 30 K. In dotted lines are shown simulations of spectra (a) and (b) respectively. (c) Enzyme from *D. fructosovorans*, Ni-C species, 80 μM. (d) Spectrum recorded after illumination of same for 120 min at 30 K. (e) Enzyme from *Dm. baculatum*, Ni-C concentration, 53 μM. (f) Spectrum obtained after the illumination of (e) for 3 min at 30 K. Conditions of measurement: temperature 30 K, microwave power 2 mW, modulation amplitude 1.0 mT, microwave frequency (a,b) 9.357 GHz, (c,d), 9.359 GHz and (e,f) 9.352 GHz. Spectra for the same enzyme were recorded with the same receiver gain.

had in total the same double-integrated intensity as the corresponding dark signal. Good simulations were obtained for Ni-C, Ni-L1 and Ni-L2 EPR species, as well as for the spectra which contain different proportions of Ni-L1 and Ni-L2 species, on the assumption that they correspond to non-interacting rhombic species (Fig. 1a,b). Similar spectra (Fig. 1c,d) were obtained by photoconversion of the Ni-C state of *D. fructosovorans*. The *g*-factors (Table 1) are similar to those seen in *C. vinosum* [23] and *T. roseopersicina* [26]. For *Dm. baculatum* hydrogenase, the Ni-L1 and Ni-L2 signals had *g*-factors (Table 1; Fig. 1e,f) that were significantly different from the [NiFe]-hydrogenases, but similar to those observed for the [NiFeSe]-hydrogenase of *M. voltae* [28].

Table 1
g-factors observed for the 'dark' and 'light-induced' species of the Ni-C EPR signals in the different hydrogenases studied

Source of hydrogenase	Ni STATE	g_1	g_2	g_3
D. gigas	Ni-C	2.192	2.146	2.009
	Ni-L1	2.264	2.113	2.044
	Ni-L2	2.293	2.124	2.045
	Ni-L3	2.41	2.16	n.d.
D. fructosovorans	Ni-C	2.192	2.146	2.009
	Ni-L1	2.264	2.113	2.044
	Ni-L2	2.293	2.124	2.045
Dm. baculatum	Ni-C	2.215	2.161	2.008
	Ni-L1	2.300	2.124	2.047
	Ni-L2	2.337	2.145	2.041
	Ni-L3	2.478	2.163	2.029

Values were derived by simulation, assuming no interactions between species. n.d., not determined, due to overlap with other species.

After extensive illumination, a third light-induced signal, here referred to as Ni-L3, appeared (Fig. 2). This signal was observed with all three hydrogenases. For the [NiFe]-hydrogenases the signal had $g_1 = 2.41$ and $g_2 =$

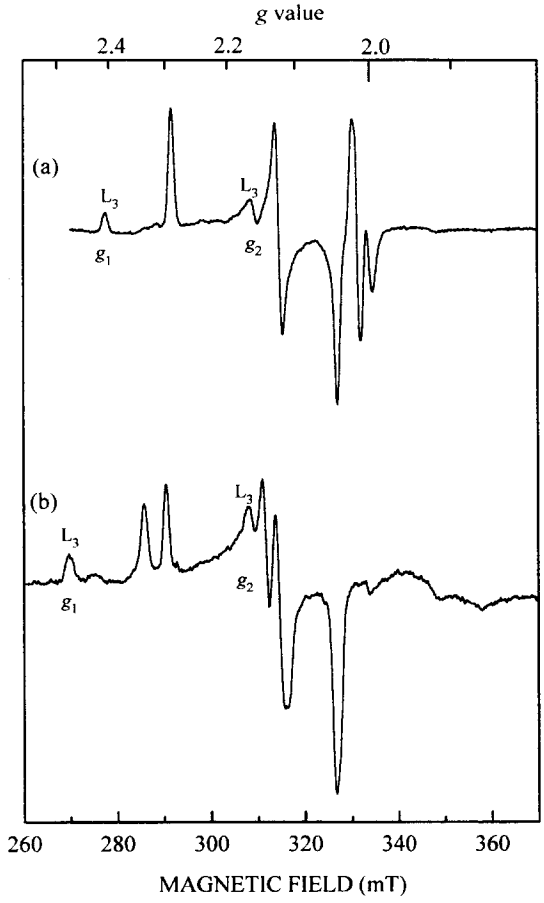

Fig. 2. Prolonged light-induced transition of the Ni-C EPR signal. (a) Enzyme from *D. gigas*, Ni-C state, illuminated for 150 min at 77 K. (b) Enzyme from *Dm. baculatum*, Ni-C state illuminated for 150 min at 30 K. Conditions of measurement as for Fig. 1, except microwave frequency, (a), 9.357, (b) 9.352 GHz.

2.16, g_3 being undetectable, probably due to superposition of g_3 of the Ni-L1 and Ni-L2 signals. The values for this signal in *D. baculatum* hydrogenase were slightly different, $g = 2.48, 2.16, 2.03$.

3.2. Rates of interconversion of the photochemically-induced states

At temperatures below 60 K, upon further illumination of *D. gigas* hydrogenase, or more slowly in the dark, the Ni-L1 signal disappeared and was replaced by Ni-L2 (Fig. 3A). At 60 K, light irradiation of the Ni-C form induced traces of Ni-L1 that disappeared almost immediately ([35], cf. Fig. 6 herein). Increasing the temperature above 60 K induced rapid conversion of the Ni-L1 signal into the Ni-L2 signal. No major differences were found in the kinetics of photoconversion of the Ni-C species and dark conversion of Ni-L1 into Ni-L2 at temperatures between 5 and 30 K (Table 2). The different behaviour of the two overlapping light-induced signals demonstrates that after illumination of the Ni-C species, two different kinds of nickel species are present. The differences in the g-factors imply subtly different coordination environments. One of the species (Ni-L1) may be an intermediate in the formation of the other one (Ni-L2), at least at low temperatures. After raising the temperature in the dark to 140 K for 40 min, the Ni-C signal reappeared with the original intensity. Hence both Ni-L1 and Ni-L2 are unstable states relative to Ni-C. Ni-L3 was also observed to revert to Ni-C at temperatures above 120 K.

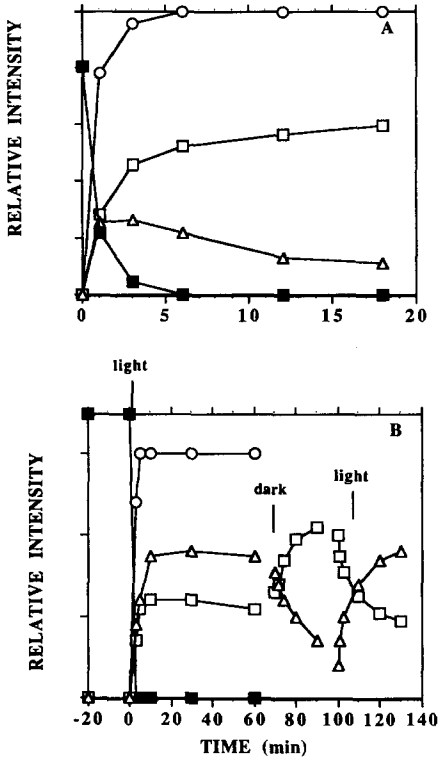

Fig. 3. Time course of the light-induced changes observed in the Ni-C EPR signals. (A) H_2-reduced *D. gigas* hydrogenase. (B) H_2-reduced *Dm. baculatum* hydrogenase. Changes observed upon illumination in H_2O at 30 K for the (■) g_1 component of the Ni-C signal, (△) g_1 component of the Ni-L1 signal, (□) g_1 component of the Ni-L2 signal, and (O) g_3 component of the Ni-L signal. The signals have been normalized.

Table 2
$t_{1/2}$ of the photoconversion of Ni-C EPR signal into the 'light-induced' states

Source of hydrogenase	Solvent	Temperature	$t_{1/2}$ (min)
D. gigas	H_2O	5 K	1
	H_2O	30 K	1
	H_2O	60 K	1.2
	^2H_2O	30 K	30
D. fructosovorans	H_2O	30 K	5
	^2H_2O	30 K	10
Dm. baculatum	H_2O	30 K	1.8
	^2H_2O	30 K	2

$t_{1/2}$ values are the times required for the half-maximum appearance of the total illuminated states, estimated by the amplitude of the g_3 peak. The $t_{1/2}$ values are approximate, since they depend on the absorbance and turbidity of the frozen samples. For consistency of comparison, samples were prepared at similar protein concentrations, in the same buffer, and frozen in the same way.

For *D. fructosovorans* periplasmic hydrogenase, the rate of conversion at 30 K of Ni-C to the illuminated states was 5-fold slower than for *D. gigas* (Table 2). It is important to note that $t_{1/2}$ values are approximate, since changes of the solution opacity can modify the quantum yield and distort the $t_{1/2}$ values and their comparison. Nevertheless, since enzymes were similar in concentration for all the samples and the optical path was short, the error in the determination of the $t_{1/2}$ values is not expected to exceed $\pm$ 15%. Raising the temperature of a sample illuminated at temperatures below 60 K induced rapid conversion of the Ni-L1 signal into the Ni-L2 signal. Light irradiation of the Ni-C species at temperatures above 60 K induced only signal Ni-L2 (not shown). The photoconversion was reversible at temperatures above 120 K.

For *Dm. baculatum* hydrogenase, the rate of photoconversion of the Ni-C state at 30 K was comparable with that of *D. gigas*. On further illumination at temperatures below 40 K the Ni-L1 signal was not completely converted into Ni-L2, as found for the *D. gigas* and *D. fructosovorans* enzymes, but an equilibrium mixture of the two species was generated (Fig. 3B). In the dark, Ni-L1 was observed to convert into Ni-L2, but upon re-illumination, Ni-L2 tended to revert to Ni-L1 and the equilibrium was re-established. At temperatures between 40 and 100 K, the species were rapidly converted into Ni-L2. Above 100 K, they reverted to Ni-C. For *Dm. baculatum* hydrogenase conversion of Ni-L3 into Ni-L2 was also observed upon warming the sample over 40 K.

3.3. Isotopic effects on the photoilluminated Ni-C signal

Isotopic substitution had a drastic effect on the rate of photoconversion of the Ni-C signal of *D. gigas* hydrogenase. The rate of conversion at 30 K to the light-induced signals in ^2H_2O was 30-times slower than that in H_2O (Table 2). The rate of photoconversion was similar at temperatures between 4.2 and 30 K. The photoeffect caused the disappearance of the split Ni-C signal and the simultaneous appearance of two overlapping signals, apparently similar to those obtained for the sample in H_2O [35]. Further illumination of the enzyme at 5 or 30 K, or just maintaining the sample in the dark at these temperatures, induced the conversion of the Ni-L1 signal into the Ni-L2, this process being slower than for the sample in H_2O.

For *D. fructosovorans* periplasmic hydrogenase, the rate of conversion of the Ni-C species to the light-induced species at 30 K was 5-fold times slower than for *D. gigas*. The rate of transition at 30 K of Ni-C to Ni-L in the ^2H_2O samples was 2 times slower than of that in H_2O (Table 2).

For *Dm. baculatum* hydrogenase, replacement of H_2O by ^2H_2O had almost no effect on the rate of photoconversion of the Ni-C signal at 5 or 30 K (Table 2), but it had a considerable effect on the rate of interconversions of Ni-L1 and Ni-L2. Further illumination of the enzyme, at either 5 K or 30 K, did not induce the conversion of the Ni-L1 species into Ni-L2; upon stopping illumination, the rate of the conversion of the Ni-L1 signal into Ni-L2 was several orders of magnitude slower than in H_2O at the temperatures assayed (not shown). Upon a second illumination cycle, conversion of Ni-L2 into Ni-L1 was 4-fold slower than for the samples in H_2O.

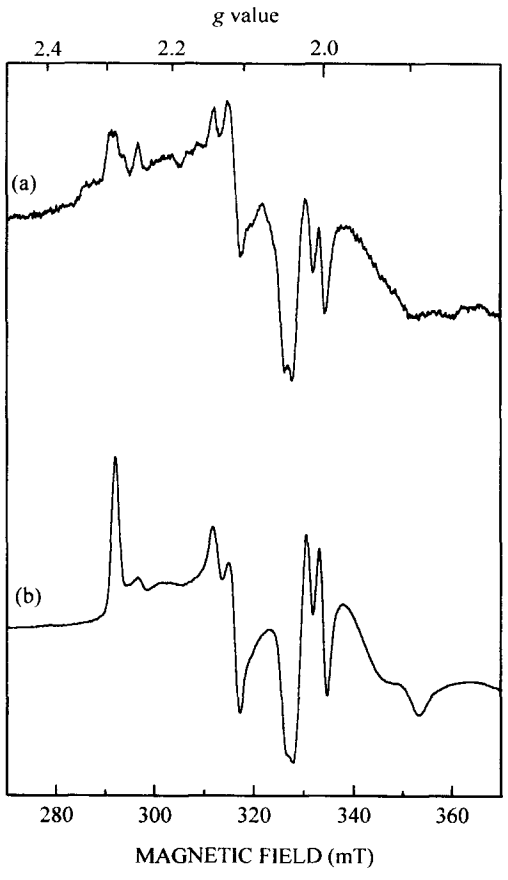

Fig. 4. Interactions of the illuminated species with [4Fe-4S] clusters. Spectra of Ni-C species after illumination at 5 K. (a) *D. gigas*. (b) *D. fructosovorans*. EPR conditions; Spectra were recorded at 5 K, with microwave frequency, (a), (b) 9.358, 9.359 GHz, microwave power 2 mW, modulation amplitude 1.0 mT.

3.4. Interactions with [4Fe-4S] clusters

As already noted, if the redox potential is adjusted so that the [4Fe-4S] clusters are predominantly reduced, the Ni-C spectrum shows a splitting at temperatures below 10 K, due to static electron spin-spin interactions [7,22]. When *D. gigas* hydrogenase in this state was illuminated and examined at temperatures below 10 K, the split Ni-C signal disappeared and new photochemically generated signals appeared [35]. The new spectrum (Fig. 4) is due to the superposition of at least three spectra, one of them due to the broad, fast-relaxing reduced [4Fe-4S] cluster signal and the two overlapping photoilluminated Ni-L signals (Fig. 4a). Further illumination of the enzyme at 5 K, or just incubation in the dark, induced the disappearance of the 'split' Ni-L1 signal and conversion into 'split' Ni-L2. These signals were deconvoluted by subtraction of spectra containing different proportions of the photoilluminated Ni-L signals [35].

Like the Ni-C signal [22], these signals are split by spin-spin interactions with a nearby paramagnet, probably one of the [4Fe-4S] clusters. Accurate information about exchange and dipolar splittings requires measurements at multiple frequencies and complex simulations [22] which were not attempted in the present study. Approximate values for the splittings were derived on the assumption of a dipolar interaction; these are listed in Table 3. They show that the interactions are anisotropic, and different for the two species. In the Ni-L1 signal the greatest splitting was on g_1 feature, while in Ni-L2 the greatest splitting was on the g_2 feature.

For *D. fructosovorans* hydrogenase, although the spectra of the Ni-L1 and Ni-L2 species were almost identical to *D. gigas*, the anisotropy of the paramagnetic splitting was different (Fig. 4, Table 3). The splittings were noticeably smaller for the g_1 component of the Ni-L1 and Ni-L2 species, and slightly larger for the g_2 and g_3 components of the Ni-L2 species. The most likely explanation of this is that the axis of the dipolar interaction with the paramagnet has a different orientation relative to the principal axes of the g-matrix. Alternatively, the difference between the split Ni-L2 signals of *D. gigas* and *D. fructosovorans* hydrogenases could be due to an earlier collapse of the g_1 lines of the *D. fructosovorans* enzyme, due to a shorter

Table 3
Approximate increases in linewidths of the Ni-C and NI-L signals, due to interactions with [4Fe-4S] clusters

Source of hydrogenase	Ni state	Linewidth increases at g_1 mT	(MHz)	g_2 mT	(MHz)	g_3 [a] mT	(MHz)
D. gigas	Ni-C	7	(215)	16.5 [c]	(500) [c]	5.7 [c]	(160) [c]
	Ni-L1	2.6	(82)				
	Ni-L2	1.1	(35)	2.8	(83)	1.8	(51)
	Ni-L3	2.1	(71)	9.5	(290)	n.d.	
D. fructosovorans	Ni-C	7.2	(223)	17 [c]	(513) [c]	6.3 [c]	(178) [c]
	Ni-L1	1.8 [b]	(57) [b]				
	Ni-L2			3.8	(113)	2.3	(65)
Dm. baculatum	Ni-C	7	(217)	16 [c]	(481) [c]	3.5 [c]	(100) [c]
	Ni-L1	≈ 4	(≈ 130)				
	Ni-L2	0 [b]	(0) [b]	4.4 [b]	(132) [b]	3.4	(97)
	Ni-L3					n.d.	

Estimated from the spectra recorded at 5 K, assuming an anisotropic dipolar splitting, and excluding exchange coupling effects.
[a] Data at g_3 are less accurate due to overlapping with strong reduced [4Fe-4S] signal.
[b] Spectral splitting not observed, but linewidth is broadened.
[c] No splitting detected.

spin-lattice relaxation time (T_1) for the [4Fe-4S] clusters in this enzyme.

The splitting of the Ni-L2 signal, as with the Ni-C signal [7,36] broadened out as the temperature was raised. The g_1 feature, with the smallest splitting, broadened out first, and the g_2 feature, with the largest splitting, broadened out last. This is to be expected as the broadening occurs when the splitting (in MHz) is comparable with the electron spin relaxation rate T_l (in MHz). The condition for this is

$$1/T_1 > \Delta B \cdot g \cdot \mu_B/h$$

where ΔB is the splitting in magnetic field units, g is the g-factor, μ_B is the Bohr magneton and h is Planck's constant.

For *Dm. baculatum* hydrogenase, the nickel signals were more difficult to observe at low temperatures, owing to overlap with the intense spectrum from the [4Fe-4S] centres, which is not as broad as in the other nickel-containing enzymes. However, the effects were qualitatively similar to those for the [NiFe]-hydrogenases. In the Ni-L1 signal the most significant splitting was on g_1, whereas in the Ni-L2 signal, greater splittings were observed on g_2 and g_3 (Table 3).

The interactions with the iron-sulphur cluster were also observed in the low field feature of the Ni-L3 signal which was induced at low temperatures (Fig. 5; Table 3). This

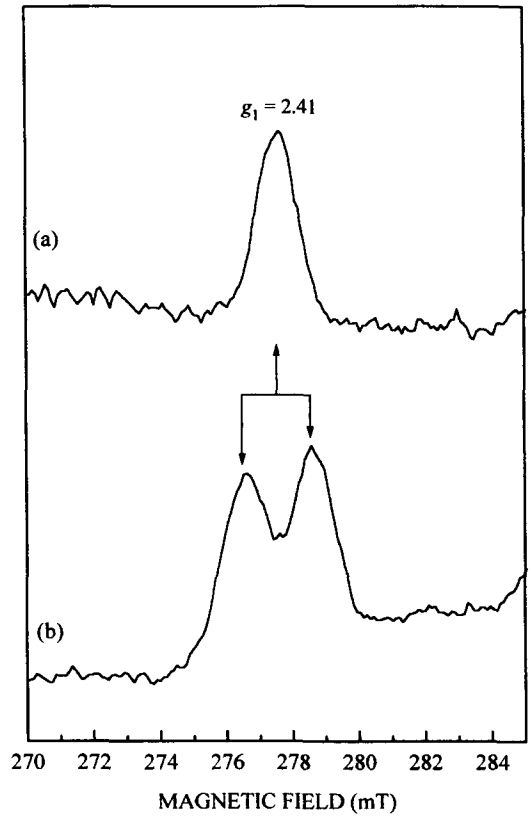

Fig. 5. Detail of the low-magnetic field region after prolonged illumination of the Ni-C EPR signal of D. gigas hydrogenase. The enzyme was illuminated at 77 K for 150 min and spectra recorded at (a) 30 K and at (b) 5 K. EPR conditions; Microwave frequency, 9.359 GHz. Microwave power 2 mW, modulation amplitude 1.0 mT.

Table 4
Proton couplings estimated from linewidth increments in H_2O of the Ni-C signals

Source of hydrogenase	Coupled protons	$A_H{}^a(g_1)$ (MHz)	$A_H{}^a(g_2)$ (MHz)	$A_H{}^b(g_1)$ (MHz)	$A_H{}^b(g_2)$ (MHz)	σ^2
D. gigas	1 proton	19.0	15.7			0.00027
	2 equivalent protons	13.0	10.2			0.000271
	2 non equivalent protons *	14.0	16.8 *	14.9	4.4 *	0.000259
D. fructosovorans	1 proton	18.2	12.7			0.000235
	2 equivalent protons	12.1	8.3			0.000235
	2 non equivalent protons fixing $A_{H(g_2)}$ to data *	13.6	16.8 *	13.0	4.4 *	0.00024

Values from simulation assuming coupling to protons. Simulations were performed assuming either one or two equivalent protons (a), or two different protons (a, b) with the couplings measured in ENDOR by Fan et al. [24] at g_2. Couplings have been estimated at g_1 and g_2 of the Ni-C spectrum. σ^2, represents the value of the mean square deviation between experimental and simulated spectra.
* Hyperfine couplings from ENDOR [24].

effect was observed in the [NiFe]- and [NiFeSe]-hydrogenases, which confirms that this signal is produced by nickel which is still interacting with a [4Fe-4S] cluster.

3.5. Hyperfine splittings with exchangeable protons

Differences in the linewidths of the Ni-C signal were observed when *D. gigas* hydrogenase was prepared in ^2H_2O, as previously noted [23]. The linewidths of the g_1 and g_2 lines of the Ni-C signal, measured at X-band and S-band frequencies, were observed to be narrower in ^2H_2O. The hyperfine couplings were estimated by simulation (Table 4). Acceptable fits could be obtained by assuming either one or two equivalent protons, or with two different protons with the couplings measured in ENDOR spectroscopy [25]. Similar hyperfine couplings were observed for the Ni-C signal of *D. fructosovorans* hydrogenase. However, for the *Dm. baculatum* hydrogenase, no significant differences were detected in the linewidths of the Ni-C signal in ^2H_2O as compared with H_2O. For the light-induced signals Ni-L1, Ni-L2 and Ni-L3, no significant differences were observed for the *g*-factors and linewidths in ^2H_2O as compared with H_2O.

4. Discussion

The light sensitivity of the Ni-C state, yielding two or more different photochemically-induced species at temperatures below 60 K [23,35] appears to be a general property of [NiFe]-hydrogenases. An exception is a hydrogenase from *M. thermoautotrophicum*, where only one photo-induced state was reported [37]. The Ni-L1, Ni-L2 and Ni-L3 signals appear to represent different types of nickel site, with different conformations or environments. The ratio of the signals produced bears no obvious relation to the ratio of the different Ni-A and Ni-B signals observed in the oxidized enzyme.

Significant differences were found in the kinetics of the photoconversion of Ni-C in different hydrogenases, which indicates different photochemical yields for the reactions. The process was 5-times slower for the *D. fructosovorans* enzyme than for *D. gigas*. These differences may be related to subtle differences in the coordination sphere of nickel in the Ni-C state of the enzyme.

The interconversions between the different states are summarized in Scheme 1. The changes in the spectra that occurred on annealing in the dark give an indication of the relative energy levels of the photo-induced nickel states. Thus the observation that the Ni-L1 species decayed into the Ni-L2 species indicates that the Ni-L1 state is higher in energy, and that the Ni-L1 species is an intermediate in the formation of the Ni-L2 species, at least at low temperatures. All three light-induced forms, Ni-L1, Ni-L2 and Ni-L3 reverted to Ni-C at temperatures above 120 K, and are thus higher in energy than the Ni-C state.

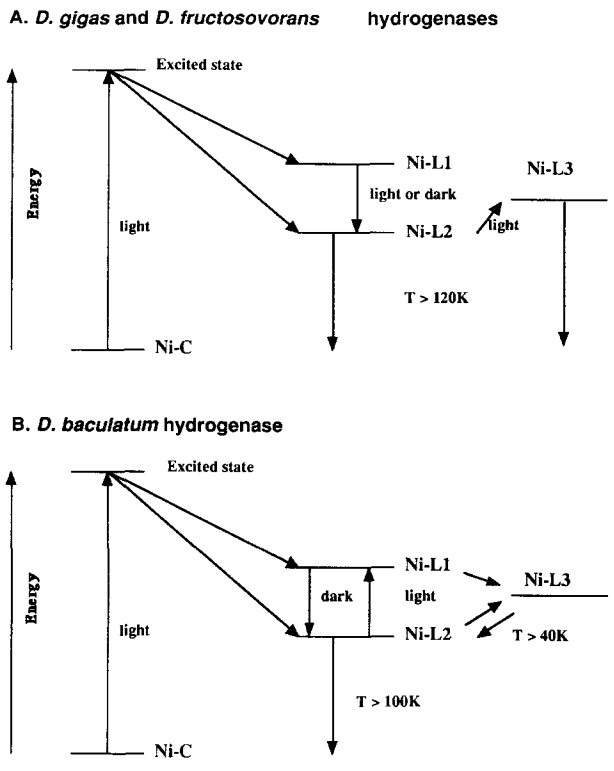

Scheme 1. 'Light–dark' transitions of the Ni-C and Ni-L species of the different hydrogenases.

The temperatures required for the interconversions of the different Ni-L species give an indication of the relative energy barriers to the conversions. Increasing the temperature above 60 K induced rapid conversion of the Ni-L1 species into Ni-L2, but the Ni-L2 species did not revert to Ni-C unless the temperature was above 100 K. Therefore the energy barrier for the conversion of the Ni-L1 species into Ni-L2 is lower than that for the conversion of Ni-L2 into Ni-C. In *D. gigas* and *D. fructosovorans* hydrogenases Ni-L3 converted to Ni-C only at temperatures above 100 K, whereas in *Dm. baculatum* hydrogenase, conversion of Ni-L3 into Ni-L2 was observed above 40 K. In *T. roseopersicina* hydrogenase it was was reported that conversion of the light-induced species to Ni-C occurred at 194 K [26]. Some conversion was observed at much lower temperatures.

Not only the Ni-C species, but also the Ni-L1 and Ni-L2 species are able to capture light energy and undergo photochemical reactions. Light irradiation of the Ni-L1 species of *D. gigas* and *D. fructosovorans* hydrogenases enhanced the conversion into Ni-L2. By contrast, irradiation of Ni-L2 in *Dm baculatum* hydrogenase led to reconversion to Ni-L1. After extensive illumination of hydrogenases giving the the Ni-L2 signals, the Ni-L3 species appeared.

Isotopic effects, due to the introduction of deuterium, have been found for the kinetics of photodissociation of all the [NiFe]-hydrogenases studied so far. We could not

detect this effect in the [NiFeSe]-hydrogenase of *Dm. baculatum*, although an isotope effect on photodissociation has been reported for another [NiFeSe]-hydrogenase, from *M. voltae* [38]. By contrast, significant kinetic isotope effects were observed in the photoconversion of the Ni-L1 species of *Dm. baculatum* hydrogenase into Ni-L2, and of Ni-L2 into Ni-L1 in a second illumination cycle after keeping the illuminated sample in the dark. The isotopic effects imply that the rates of the illumination processes are determined, at least in part, by the movement of a hydrogen nucleus [23]. The two different forms represented by the Ni-L1 and Ni-L2 signals might therefore represent different locations for this hydrogen. The conversion of Ni-L1 into Ni-L2 in the dark was apparently temperature-independent below 30 K. This is indicative of a non-thermal process which probably involves proton tunnelling; this involves proton movements over distances of the order of 0.1 nm [39,40].

The EPR spectra of all three light-induced signals Ni-L1, Ni-L2 and Ni-L3, like Ni-C, showed splittings when recorded at temperatures below 20 K, due to interactions with another paramagnet, presumably a [4Fe-4S] centre. Different splittings have been observed for g_1, g_2 and g_3 of the Ni-L2 spectrum, indicating that, in the illuminated state, coupling between the nickel and the [4Fe-4S] cluster is anisotropic. Thus it should be possible to derive information about the orientation of the axes of the *g*-matrix relative to the Ni-[4Fe-4S] axis (Guigliarelli et al., to be published).

Van der Zwaan et al. [41] showed that a paramagnetic state of reduced *C. vinosum* hydrogenase treated with CO, a competitive inhibitor, was also photosensitive. This species showed a strong hyperfine splitting with ^{13}CO and was assigned as a Ni^{I}-carbonyl. Significantly, the EPR signal of the photoproduct was virtually identical to that of photolyzed Ni-C, also showing the presence of two illuminated species. No difference was detected for the kinetics of these processes in $^{2}H_2O$, indicating that hydrogen might bind as a hydride ion, and CO can bind to the nickel atom at the same position [42]. Another EPR-silent carbonyl species, formed by treatment with CO, has been interpreted as the higher oxidation state, Ni^{II}-CO. Infrared studies on this state have shown that it is also photolabile at cryogenic temperatures and that it rebinds to form the original carbon monoxy species at temperatures above 200 K [43].

The possibility that the photoconversion of Ni-C involves the photolysis of a nickel-hydride or nickel-dihydrogen species has been discussed by a number of authors [7,23,26,28]. However, in view of the undetectable, and therefore less than 10 MHz, hyperfine broadening by exchangeable hydrons in the [NiFeSe]-hydrogenase of *D. baculatum* and *M. voltae*, it is difficult to envisage a direct coordination of hydrogen to the nickel in the Ni-C state. Even if the coordination geometry allowed very little orbital overlap, the anisotropic dipolar interaction would be expected to produce a splitting substantially greater than this, on at least one of the *g*-factor components. The absence of a hydride on the Ni-C state does not preclude the possibility of such a species in the lower, EPR-silent oxidation state which is obtained by further reduction of this form of the enzyme. It has been demonstrated that in hydrogenases from *M. themoautotrophicum*, *C. vinosum* and *D. gigas*, in the absence of electron mediators, the Ni-C state is stable in solution, persists upon removal of hydrogen and does not release dihydrogen [44,45]. Therefore, the Ni-C state is not the species which spontaneously reduces protons to H_2, and a second site for reaction with hydrogen is proposed [44]

For the Ni-L signals, unlike the Ni-A, Ni-B and Ni-C signals, the lowest *g*-factor is considerably greater than 2.0. This has been taken as evidence that the unpaired electron has moved from an orbital which is predominantly d_{z^2} in character, to another orbital such as $d_{x^2-y^2}$ [23,28]. The changes in the electronic axis upon illumination of the Ni-C state and the carbon monoxide complex [42] have suggested models for the coordination of the nickel in the Ni-C state in hydrogenase [28]. A modified model has been proposed after studies with ^{77}Se-enriched [NiFeSe]-hydrogenase [38]. However, these proposals may have to be reconsidered in the light of the model for the site derived from X-ray crystallography of *D. gigas* hydrogenase [15]. This model suggest that the nickel is bound by four cysteine sulphurs, one of which is substituted by selenocysteine in the [NiFeSe]-hydrogenases, and at least one other ligand, possibly water. Two of the cysteine ligands appear to bridge to another metal ion, probably iron. Close to the metal sites there are at least two basic groups, a histidine and an arginine. In such a structure there are numerous potential sites for the hydrons and carbon monoxide to bind. It should be noted that the form which was crystallized was in the unready state, so further work is needed to determine the geometry of the nickel-containing site in the active enzyme.

Acknowledgements

We thank Dr. Ruth Williams for assistance, discussions and advice, and Andrew White for technical assistance. The work was supported by a Fellowship fron the European Union to M.M., and grants from the U.K. Biotechnology and Science and Engineering Research Council and the European Union to R.C.

References

[1] Adams, M.W.W. (1990) Biochim. Biophys. Acta 1020, 115–145.
[2] Cammack, R., Fernandez, V.M. and Hatchikian, E.C. (1994) Methods Enzymol. 243 43–68.
[3] Albracht, S.P.J. (1994) Biochim. Biophys. Acta 1188, 167–204.

[4] Wu, L.F. and Mandrand, M.A. (1993) FEMS Microbiol. Rev. 104, 243–270.
[5] Hatchikian, E.C., Fernandez, V.M. and Cammack, R. (1990) in Microbiology and Biochemistry of Strict Anaerobes Involved in Interspecies Hydrogen Transfer (Bélaich, J.-P., Bruschi, M. and Garcia, J.-L., eds.), pp. 53–75. Plenum Press, New York.
[6] Przybyla, A.E., Robbins, J., Menon, N. and Peck, H.D., Jr. (1992) FEMS Microbiol. Rev. 88, 109–136.
[7] Cammack, R., Patil, D.S., Hatchikian, E.C. and Fernandez, V.M. (1987) Biochim. Biophys. Acta 912, 98–109.
[8] Teixeira, M., Moura, I., Xavier, A.V., Moura, J.J.G., LeGall, J., DerVartanian, D.V., Peck, H.D., Jr. and Huynh, B.H. (1989) J. Biol. Chem. 264, 16435–16450.
[9] Patil, D.S. (1994) Methods in Enzymol. 243, 68–94.
[10] He, S.H., Teixeira, M., LeGall, H., Patil, D.S., Moura, I., Moura, J.J.G., DerVartanian, D.V., Huynh, B.H. and Peck, H.D., Jr. (1989) J. Biol. Chem. 264, 2678–2682.
[11] Eidsness, M.K., Scott, R.A., Prickril, B.C., DerVartanian, D.V., LeGall, J., Moura, I., Moura, J.J.G. and Peck, H.D., Jr. (1989) Proc. Natl. Acad. Sci. USA 86, 147–151.
[12] Sorgenfrei, O., Linder, D., Karas, M. and Klein, A. (1993) Eur. J. Biochem. 213, 1355–1358.
[13] Hatchikian, E.C., Bruschi, M. and LeGall., J. (1978) Biochem. Biophys. Res. Commun. 82, 451–461.
[14] Niviere, V., Hatchikian, E.C., Cambillau, C. and Frey, M. (1987) J. Mol. Biol. 195, 969–971.
[15] Volbeda, A., Charon, M.H., Piras, C., Hatchikian, E.C., Frey, M. and Fontecilla-Camps, J.C. (1995) Nature 373, 580–587.
[16] Voordouw, G. (1992) in Advances in Inorganic Chemistry (Cammack, R. and Sykes, A.G., eds.), Vol. 38, pp. 397–422, Academic Press, New York.
[17] Moura, J.J.G., Moura, I., Huynh, B.H., Krüger, H.-L., Teixeira, M., DuVarney, R.C., DerVartanian, D.V., Xavier, A.V., Peck, H.D., Jr. and LeGall, J. (1982) Biochem. Biophys. Res. Commun. 108, 1388–1393.
[18] Lancaster, J.R., Jr. (1980) FEBS Lett. 115, 285–288.
[19] Fernandez, V.M., Hatchikian, E.C., Patil, D.S. and Cammack, R. (1986) Biochim. Biophys. Acta 883, 145–153.
[20] Kojima, N., Fox, J.A., Hausinger, R.P., Daniels, L., Orme-Johnson, W.H. and Walsh, C.T. (1983) J. Biol. Chem. 80, 378–382.
[21] Cammack, R., Hall, D.O. and Rao, K.K. (1985) in Microbial Gas Metabolism: Mechanistic, Metabolic and Biotechnological Effects (Poole, R.K. and Dow, C., eds.), pp. 75–102. Academic Press, New York.
[22] Guigliarelli, B., More, C., Fournel, A., Asso, M. Hatchikian, E.C., Williams, R., Cammack, R. and Bertrand, P. (1995) Biochemistry 34, 4781–4790.
[23] Van der Zwaan, J.W., Albracht, S.P.J., Fontijn, R.D. and Slater, E.C. (1985) FEBS Lett. 179, 271–277.
[24] Chapman, A., Cammack, R., Hatchikian, E.C., McCracken, J. and Peisach, J. (1988) FEBS Lett. 242, 134–138.
[25] Fan, C.L., Teixeira, M., Moura, J.J.G., Moura, I., Huynh, B.H., LeGall, J., Peck, H.D., Jr. and Hoffman, B.M. (1991) J. Am. Chem. Soc. 113, 20–24.
[26] Whitehead, J.P., Gurbiel, R.J., Bagyinka, C., Hoffman, B.M. and Maroney, M.J. (1993) J. Am. Chem. Soc. 115, 5629–5635.
[27] Cammack, R., Bagyinka, C. and Kovacs, K.L. (1989) Eur. J. Biochem. 182, 357–362.
[28] Sorgenfrei, O., Klein, A. and Albracht, S.P.J. (1993) FEBS Lett. 332, 292–297.
[29] Rousset, M., Dermoun, Z., Wall, J.D. and Belaich, J.P. (1993) J. Bacteriol. 175, 3388–3393.
[30] Hatchikian, E.C., Traore, A.S., Fernandez, V.M. and Cammack, R. (1990) Eur. J. Biochem. 187, 635–643.
[31] Bell, S.H., Dickson, D.P.E., Rieder, R., Cammack, R., Patil, D.S., Hall, D.O. and Rao, K.K. (1984) Eur. J. Biochem. 145, 645–651.
[32] Rieder, R., Cammack, R. and Hall, D.O. (1984) Eur. J. Biochem. 145, 637–643.
[33] Cammack, R., Patil, D.S., Aguirre, R. and Hatchikian, E.C. (1982) FEBS Lett. 142, 289–292.
[34] Cammack, R. and Cooper, C.E. (1993) Methods in Enzymology 227, pp. 353–384.
[35] Medina, M., Williams, R., Hatchikian, E.C. and Cammack, R. (1994) J. Chem. Soc. Faraday Trans. 90, 2921–2924.
[36] Teixeira, M., Moura, I., Xavier, A.V., Huynh, B.H., DerVartanian, D.V., Peck, H.D., Jr., LeGall, J. and Moura, J.J.G., (1985) J. Biol. Chem. 260, 8942–8950.
[37] Van der Zwaan, J.W., Albracht, S.P.J., Fontijn, R.D. and Mul, P. (1987) Eur. J. Biochem. 169, 377-384.
[38] Sorgenfrei, O., Duin, E.C., Albracht, S.P.J. and Klein, A. (1994) IV International Conference on the Molecular Biology of Hydrogenases. pp 135.
[39] Cha, Y., Murray, C.J. and Klinman, J.P. (1989) Science 243, 1325–1330.
[40] Rucker, J., Cha, Y., Jonsson, T., Grant, K.L. and Klinman, J.P. (1992) Biochemistry 31, 11489–11499.
[41] Van der Zwaan, J.W., Coremans, J.M.C.C., Bouwens, E.C.M. and Albracht, S.P.J. (1990) Biochim. Biophys. Acta 1041, 101–110.
[42] Van der Zwaan, J.W., Albracht, S.P.J., Fontijn, R.D. and Roelofs, Y.B.M. (1986) Biochim. Biophys. Acta 872, 208–215.
[43] Bagley, K.A., Van Garderen, C.J., Chen, M., Duin, E.C., Albracht, S.P.J. and Woodruff, W.H. (1994) Biochemistry 33, 9229–9236.
[44] Coremans, J.M.C.C., Van Garderen, C.J. and Albracht, S.P.J. (1992) Biochim. Biophys. Acta 1119, 148–156.
[45] Barondeau, D.P., Roberts, L.M. and Lindahl, P.A. (1994) J. Am. Chem. Soc. 116, 3442–3448.